Hindawi Publishing Corporation
EURASIP Journal on Advances in Signal Processing
Volume 2008, Article ID 365021, 10 pages
doi:10.1155/2008/365021

Research Article

An Adaptively Accelerated Lucy-Richardson Method for Image Deblurring

Manoj Kumar Singh,[1] Uma Shanker Tiwary,[2] and Young-Hoon Kim[1]

[1] *Sensor System Laboratory, Department of Mechatronics, Gwangju Institute of Science and Technology (GIST), 1 Oryong-dong, Buk-gu, Gwangju 500 712, South Korea*
[2] *Indian Institute of Information Technology Allahabad (IIITA), Deoghat Jhalwa, Allahabad 211012, India*

Correspondence should be addressed to Young-Hoon Kim, yhkim@gist.ac.kr

Received 11 June 2007; Accepted 3 December 2007

Recommended by Dimitrios Tzovaras

We present an adaptively accelerated Lucy-Richardson (AALR) method for the restoration of an image from its blurred and noisy version. The conventional Lucy-Richardson (LR) method is nonlinear and therefore its convergence is very slow. We present a novel method to accelerate the existing LR method by using an exponent on the correction ratio of LR. This exponent is computed adaptively in each iteration, using first-order derivatives of the deblurred image from previous two iterations. Upon using this exponent, the AALR improves speed at the first stages and ensures stability at later stages of iteration. An expression for the estimation of the acceleration step size in AALR method is derived. The superresolution and noise amplification characteristics of the proposed method are investigated analytically. Our proposed AALR method shows better results in terms of low root mean square error (RMSE) and higher signal-to-noise ratio (SNR), in approximately 43% fewer iterations than those required for LR method. Moreover, AALR method followed by wavelet-domain denoising yields a better result than the recently published state-of-the-art methods.

1. INTRODUCTION

Image deblurring is a longstanding linear inverse problem and is encountered in many applications such as remote sensing, medical imaging, seismology, and astronomy. Generally, many linear inverse problems are ill-conditioned since either inverse of the linear operators does not exist or is nearly singular, giving highly noise sensitive solutions. In order to deal with ill-conditioned nature of these problems, a large number of linear and nonlinear methods have been developed. Most linear methods are based on the regularization (see [1, 2]) while nonlinear methods are developed under Bayesian's framework and are solved iteratively (LR, maximum entropy, Landweber) [1–8]. The nonlinear methods under Bayesian-wavelet framework have been reported recently (e.g., see [9, 10]). The main drawbacks of these nonlinear methods are slow convergence and high-computational cost.

The simplicity and ease in implementation and computation of LR method make it preferable among all the nonlinear methods for many applications. Many techniques for accelerating the LR method have been given by different researchers [3, 11–16]. All of these methods use additive correction term which is computed in every iteration and added to the result obtained in previous iteration. In most of these methods, the correction term is obtained by multiplying an estimate of gradient of objective function with an acceleration parameter. One method that uses line search approach [12] adjusts acceleration parameter to maximize the log-likelihood function at each iteration and uses the Newton-Raphson iteration to find its new value. It speeds up the conventional LR method by a factor of $2 \sim 5$, but requires a prior limit on acceleration parameter to prevent the divergence. In the steepest ascent method [13], the acceleration is achieved by maximizing a function in the direction of the gradient vector. The main problem with gradient-based methods, such as steepest ascent and steepest descent, is the selection of optimal acceleration step. Large acceleration step speeds up the algorithms, but it may introduce error. If the error is amplified during iteration, it can lead to instability.

A gradient search method proposed in [14–16] known as conjugate gradient (CG) method is better than the steepest ascent method. The CG method requires gradient of the objective function and an efficient line search technique. However, for the exact maximization of objective function, this method requires additional function evaluations taking significant computation time. Another class of acceleration methods, based on statistical consideration rather than numerical overrelaxation, is discussed in [17].

One of our objectives in this paper is to give a simple and efficient method which overcomes difficulties in previously proposed methods. In order to cope with the problems of earlier accelerated methods, we propose AALR method, which requires minimum information about the iterative process. Our proposed method uses the multiplicative correction term instead of using additive correction term. The multiplicative correction term is obtained by using an exponent on the correction ratio in the LR method. This exponent is calculated adaptively in each iteration, using first-order derivatives of deblurred image from the previous two iterations. The positivity of pixel intensity in the proposed acceleration method is automatic since multiplicative correction term is always positive, while in the other acceleration methods based on additive correction term, the positivity is enforced manually at the end of each iteration. Thus, one bottleneck is removed.

Another objective of this paper is to discuss superresolution and nature of noise amplification of the proposed accelerated LR method. Superresolution means restoring the frequency beyond the diffraction limit. It is often said in the support of nonlinear methods that they have superresolution capability, but very limited analytical analysis for superresolution is available. In [18], an analytical analysis of superresolution is performed assuming that the point spread function (PSF) of the system and intensity distribution of an object have Gaussian distribution. In this paper, we present general analytical interpretation of superresolving capability of the proposed accelerated method and confirmed it experimentally.

It is a well-known fact about nonlinear methods based on maximum likelihood that the restored images begin to deteriorate after a certain number of iterations. This deterioration is due to the noise amplification from one iteration to another. Due to the nonlinearity, an analytical analysis of the noise amplification for nonlinear methods is difficult. In this paper, we investigate the process of noise amplification qualitatively for the proposed AALR.

The rest of the paper is organized as follows. Section 2 describes the observation model and the proposed AALR method. Also an expression for estimating acceleration step size in AALR method is derived. Section 3 presents analytical analysis for the superresolution and noise amplification in the proposed method. Experimental results and discussions are given in Section 4. The conclusion is presented in Section 5 which is followed by references.

2. ADAPTIVELY ACCELERATED LUCY-RICHARDSON METHOD

2.1. Observation model

Consider an original image, size $M \times N$, blurred by shift-invariant PSF, h, and corrupted by Poisson noise. Observation model for the blurring in case of Poisson noise is given as [19]

$$y \sim P((h \otimes x)(z)). \tag{1}$$

Alternatively, observation model (1) can be expressed as

$$y(z) = (h \otimes x)(z) + n(z), \tag{2}$$

where P denotes the Poisson distribution, $\otimes$ is convolution operator, z is defined on a regular $M \times N$ lattice $Z = \{m_1, m_2 : m_1 = 1, 2, \ldots, M, \mathrm{m}_2 = 1, 2, \ldots, N\}$, and n is zero-mean with variance $\mathrm{var}\{n(z)\} = (h \otimes x)(z)$.

Blurred and noisy image, y, has mean $E\{y(z)\} = (h \otimes x)(z)$ and variance $\sigma_y^2(z) = \mathrm{var}\{y(z)\} = (h \otimes x)(z)$. Thus, the observation variance, $\sigma_y^2(z)$, is signal-dependent and consequently spatially variant. For mathematical simplicity, observation model in (2) can be expressed in a matrix-vector form as follows:

$$\overline{y} = \overline{H}\overline{x} + \overline{n}, \tag{3}$$

where $\overline{H}$ is the blurring operator of size $MN \times MN$ corresponding PSF h; $\overline{x}$, $\overline{y}$, and $\overline{n}$ are vectors of size $MN \times 1$ containing the original image, observed image, and sample of noise, respectively, and are arranged in a column lexicographic ordering. The aim of image deblurring is to recover an original image, $\overline{x}$, from its degraded version $\overline{y}$.

2.2. Accelerated Lucy-Richardson method

We derive the accelerated LR method, in framework of maximum likelihood [1, 2], considering that the observed image $\overline{y}$ is corrupted by the Poisson noise. If we consider only blurring, $\overline{n}$ is zero in (3), then the expected value at the ith pixel in the blurred image is $\sum_j h_{ij}x_j$, where h_{ij} is (i, j)th element of matrix $\overline{H}$ and x_j is the jth element of vector $\overline{x}$. Because of Poison noise, the actual ith pixel value y_i in $\overline{y}$ is the one realization of Poisson distribution with mean $\sum_j h_{ij}x_j$. Thus, we have the following relation:

$$p(y_i \mid \overline{x}) = \frac{\left(\sum_j h_{ij}x_j\right)^{y_i} e^{\left(-\sum_j h_{ij}x_j\right)}}{y_i!}. \tag{4}$$

Each pixel in blurred and noisy image, $\overline{y}$, is realized by an independent Poisson process. It is important to note that the assumptions about statistical independence are acknowledged to be generally incorrect. They are made solely for the purpose of mathematical tractability. Thus, the likelihood of getting noisy and blurred image, $\overline{y}$, is given by

$$p(\overline{y}/\overline{x}) = \prod_i \left(\frac{\left(\sum_j h_{ij}x_j\right)^{y_i} e^{\left(-\sum_j h_{ij}x_j\right)}}{y_i!} \right). \tag{5}$$

An approximate solution of (3), for given observed image $\overline{y}$, is obtained by maximizing the likelihood $p(\overline{y}/\overline{x})$, or equivalently log-likelihood $\log p(\overline{y}/\overline{x})$. From (5), we have

$$L = \log p(\overline{y} \mid \overline{x}) = \sum_i \left(y_i \log \left(\sum_j h_{ij} x_j \right) - \sum_j h_{ij} x_j - \log (y_i!) \right). \quad (6)$$

Differentiating L with respect to x_i, and setting $\partial L/\partial x_i = 0$, we get the following relation:

$$\sum_i h_{ij} \left(\frac{y_i}{\sum_j h_{ij} x_j} - 1 \right) = 0. \quad (7)$$

By rearranging (7),

$$\overline{H}^T \left(\frac{\overline{y}}{\overline{H}\overline{x}} \right) = 1, \quad (8)$$

where superscript T denotes transpose of matrix. In (8), $\overline{y} \mid \overline{H}\overline{x}$ denotes the vector obtained by componentwise division of $\overline{y}$ by $\overline{H}\overline{x}$. As formulated in [4, 5], we can derive (8), without any prior information about the noise type or amount of noise. Introducing exponent q on both sides of (8), we get the relation

$$\left[\overline{H}^T \left(\frac{\overline{y}}{\overline{H}\overline{x}} \right) \right]^q = 1. \quad (9)$$

Equation (9) is nonlinear in $\overline{x}$, and it is solved iteratively. Its iterative solution in kth iteration is as follows:

$$\overline{x}^{k+1} = \overline{x}^k \left[\overline{H}^T \left(\frac{\overline{y}}{\overline{H}\overline{x}^k} \right) \right]^q. \quad (10)$$

We observed that iteration given in (10) converges only for some values of q lying between 1 and 3. Large values of q ($\leq$3) may give faster convergence but with the increased risk of instability. Small values of q (≈ 1) lead to slow convergence and reduce the risk of instability. Between these two extremes, the adaptive selection of exponent q provides means for achieving faster convergence while ensuring stability. Thus, (10) with adaptive selection of exponent q leads to the AALR method. Putting $q = 1$ in (10), we get the following equation:

$$\overline{x}^{k+1} = \overline{x}^k \left[\overline{H}^T \left(\frac{\overline{y}}{\overline{H}\overline{x}^k} \right) \right]. \quad (11)$$

Equation (11) is the same as conventional LR method [2, 4, 5].

2.3. Adaptive selection of exponent q

The choice of q in (10) mainly depends on the noise, $\overline{n}$, and its amplification during iterations. If the noise is high, a smaller value of q is selected and vice versa. Thus, convergence speed of proposed method depends on the choice of the parameter q. The drawback of this accelerated form of LR method is that the selection of exponent q has to be done manually by hit and trial [6]. We overcome this serious limitation by proposing a method in which q is computed adaptively as the iterations proceed. Proposed expression for q is as follows:

$$q(k+1) = \exp \left(\frac{\| \nabla \overline{x}^k \|}{\| \nabla \overline{x}^{k-1} \|} \right) - \left(\frac{\| \nabla \overline{x}^2 \|}{\| \nabla \overline{x}^1 \|} \right), \quad (12)$$

where $\nabla \overline{x}^k$ stands for first-order derivative of $\overline{x}^k$ and $\| \cdot \|$ denotes the L_2 norm. The main idea in using first-order derivative is to utilize the sharpness of image. Because of the blurring, the image becomes smooth, sharpness decreases, and edges are lost or become weak. Deblurring makes image nonsmooth, and increases the sharpness. Hence, the sharpness of deblurred image, $\overline{x}^k$, increases as iterations proceed. For different levels of blurs and different classes of images, it has been found by experiments that L_2 norm of gradient ratio $\| \nabla \overline{x}^k \| / \| \nabla \overline{x}^{k-1} \|$ converges to one as a number of iterations increase. Accelerated LR method emphasizes speed at the beginning stages of iterations by forcing q around three. When the exponential term in (12) is greater than three, the second term, $\| \nabla \overline{x}^2 \| / \| \nabla \overline{x}^1 \|$, limits the value of q within three to prevent divergence. As iterations increase, the second term forces q towards the value of one which leads to stability of iteration. By using the exponent, q, the method emphasizes speed at the first stages and stability at later stages of iteration. Thus, selecting q given by (12) for iterative solution (10) gives accelerated LR method for image deblurring. The positivity of pixel intensity is ensured in adaptive accelerated LR method, since correction ratio in (10) is always positive. In order to initialize the accelerated LR method, the first two iterations are computed using some fixed value of q ($1 \leq q \leq 3$). In order to avoid instability at the start of iteration, $q = 1$ is a preferable choice.

2.4. An expression for estimating acceleration step size

In iterative methods for solving nonlinear equations, successive steps trace a path towards the solution through the multidimensional space. The aim of acceleration is to move faster along this path or close to it, which can be achieved by taking larger step size. If this is possible, then the accelerated method would result in the same solution. Correction term in the proposed AALR method is multiplicative, which makes it difficult to predict the step size and its direction in each iteration of this method.

In order to estimate step in AALR, we rewrite the term $\overline{H}^T(\overline{y}/\overline{H}\overline{x}^k)$ in (10) as follows:

$$\overline{H}^T \left(\frac{\overline{y}}{\overline{H}\overline{x}^k} \right) = 1 + \overline{H}^T \overline{u}^k, \quad (13)$$

where $\overline{u}^k$ is a relative fitting error and given as

$$\overline{u}^k = \frac{(\overline{y} - \overline{H}\overline{x}^k)}{\overline{H}\overline{x}^k}. \quad (14)$$

It is observed that $|\overline{u}^k| \ll 1$ for sufficiently large k. Moreover, by the Riemann-Lebesgue lemma, it is possible to show that the sum $H^T\overline{u}^k$ in (13) has value very close to zero [2]. Raising exponent q in both sides of (13), we get

$$\left[\overline{H}^T\left(\frac{\overline{y}}{\overline{H}\overline{x}^k}\right)\right]^q = \left[1+\overline{H}^T\overline{u}^k\right]^q. \tag{15}$$

Expanding the left-hand side of (15) using Taylor series expansion and retaining only the first-order term, we arrive at the following relation:

$$\left[\overline{H}^T\left(\frac{\overline{y}}{\overline{H}\overline{x}^k}\right)\right]^q \approx 1 + q*\overline{H}^T\overline{u}^k. \tag{16}$$

Substituting (16) into (10), we get the following relation:

$$\overline{x}^{k+1} \approx \overline{x}^k + q*\overline{x}^k\overline{H}^T\overline{u}^k. \tag{17}$$

From (7) and (8), it is clear that $\overline{H}^T\overline{u}^k$ is the gradient of log-likelihood function L. Thus, the approximate step length in AALR is $q*\overline{x}^k\overline{H}^T\overline{u}^k$ in the direction of gradient of log-likelihood function.

2.5. Computational considerations

For implementation of LR and AALR methods, we exploit the shift-invariant property of the PSF. In linear shift-invariant system, convolution in spatial domain becomes pointwise multiplication in Fourier domain [20]. The 2D fast Fourier transform (FFT) algorithm is used for fast computation of convolution [20].

In the LR and the AALR methods, the evaluation of the array $\overline{H}^T(\overline{y}/\overline{H}\overline{x}^k)$ is the major task in each iteration. This has been accomplished, using FFT $\hat{h}(\xi,\eta)$, $\hat{x}^k(\xi,\eta)$ of the PSF, h, and the image corresponding $\overline{x}^k$, in four steps as follows. (1) Form $\overline{H}\overline{x}^k$ by taking inverse FFT of the product $\hat{h}(\xi,\eta)\hat{x}^k(\xi,\eta)$. (2) Replace all element less than 1 by 1 in $\overline{H}\overline{x}^k$, and form the ratio $\overline{y}/\overline{H}\overline{x}^k$ in the spatial domain. (3) Find the FFT of the result obtained in step 2, $\overline{y}/\overline{H}\overline{x}^k$, and multiply this by complex conjugate of $\hat{h}(\xi,\eta)$. (4) Take the inverse FFT of the result of step 3 and replace all negative entries by zero.

The FFT is the heaviest computation in each iteration of the LR and AALR methods. Thus, the overall algorithm complexity of these methods is $O(MN\log MN)$.

3. SUPERRESOLUTION AND NOISE AMPLIFICATION IN AALR METHOD

3.1. Superresolution

It is often mentioned that the nonlinear methods have superresolution capacity, restoring the frequency beyond the diffraction limit, without any rigorous mathematical support. In spite of the highly nonlinear nature of AALR method, we explain its superresolution characteristic qualitatively by using (17).

An equivalent expression of (17) in the Fourier domain is obtained by using convolution, correlation theorem as [20]

$$X^{k+1}(\overline{f}) = X^k(\overline{f}) + \frac{q}{MN}X^k(\overline{f}) \otimes H^*(\overline{f})U^k(\overline{f}), \tag{18}$$

where superscript $*$ denotes the conjugate transpose of a matrix; X^{k+1}, X^k, and U^k are discrete Fourier transforms of size $M\times N$ corresponding to the variable in lower case letters; and $\overline{f}$ is 2D frequency index. H is the Fourier transform of PSF and it is known as optical transfer function (OTF). The OTF is band limited, say, its upper cutoff frequency is f_C, that is, $H(\overline{f}) = 0$ for $|\overline{f}| > f_C$. In order to make the explanation of superresolution easy, we rewrite (18) as follows:

$$X^{k+1}(\overline{f}) = X^k(\overline{f}) + \frac{q}{MN}\sum_{\overline{f}'}X^k(\overline{f}')H^*(\overline{f}-\overline{f}')U^k(\overline{f}-\overline{f}'). \tag{19}$$

At any iteration, the product H^*U^k in (19) is also band limited and has the frequency support, at most as that of H. Due to the multiplication of H^*U^k by X^k and the summation over all available frequency indexes, the second term in (19) is never zero. Indeed, the inband frequency components of X^k are spread out of the band. Thus, the restored image $X^{k+1}(\overline{f})$ has frequencies beyond cutoff frequency f_C. The increase in the magnitude of spectrum, at particular iteration, is q times more than conventional LR method. Reliability of the restored frequency beyond the diffraction limit can be assured by incorporating the prior information about true object in restoration process. This leads to another class of deblurring methods based on penalized maximum likelihood.

3.2. Noise amplification

It is worth noting that complete recovery of frequencies present in true image from the observed image requires large number of iterations. But due to noisy observation, noise also amplifies as iterations increase. Hence, restored image may become unacceptably noisy and unreliable for a large number of iterations.

Noise in $(k+1)$th iteration is estimated by finding the correlation of the deviation of $X^{k+1}(\overline{f})$ from its expected value $E[X^{k+1}(\overline{f})]$. This correlation is the measure of noise and is given as follows:

$$\mu_X^{k+1}(\overline{f},\overline{f}') = E\Big[\{X^{k+1}(\overline{f}) - E[X^{k+1}(\overline{f})]\} \times \{X^{k+1}(\overline{f}') - E[X^{k+1}(\overline{f}')]\}^*\Big]. \tag{20}$$

In order to simplify (20), we assume that the correlation at two different spatial frequencies is independent, that is, vanishing correlation at two different spatial frequencies.

(a) (b) (c) (d)

Figure 1: "Cameraman" image: (a) original image; (b) noisy-blurred image: PFS 5×5 uniform box-car, BSNR = 40 dB; (c) restored image by LR corresponding maximum SNR in 355 iteartions; (d) restored image by AALR corresponding maximum SNR in 200 iterations.

Substituting X^{k+1} from (19) in (20) and using the above assumption, we get the following relation:

$$\begin{aligned} N_X^{k+1}(\overline{f}) - N_X^k(\overline{f}) &= \frac{q^2}{M^2N^2}\sum_v |H(v)|^2 |U^k(v)|^2 N_X^k(\overline{f}-v) \\ &+ \frac{2q}{MN}\sum_v \mathrm{Re}\big(H^*(v)U^k(v)\big)E\Big(|X^k(\overline{f})|^2\Big) \\ &- \frac{2q}{MN}\sum_v \mathrm{Re}\big(H^*(v)U^k(v)\big)\,|E(X^k(\overline{f}))|^2, \end{aligned} \tag{21}$$

where $N_X^k(\overline{f}) = \mu_X^k(\overline{f},\overline{f})$ represents the noise in X^k at frequency $\overline{f}$. Derivation of (21) is given in the appendix. From second and third terms of (21), it is clear that in AALR method noise amplification is signal-dependent. Moreover, noise from one iteration to the next is cumulative. Thus, using many iterations, it is not guaranteed that the restored quality of the image will be acceptable. We can find total amplified noise by summing (21) over all MN frequencies.

Table 1: Blurring PSF, BSNR, and SNR.

Experiment	Blurring PSF	BSNR [dB]	SNR [dB]
Exp1	5×5 Box-car	40	17.35
Exp2	5×5 Box-car	32.76	19.34

Table 2: SNR, iterations, and computation time in the LR and AALR [10, 21, 22] methods for Exp1.

Method	SNR (dB)	Iterations	Time (s)
LR	24.54	355	158.72
AALR	24.54	200	89.45
WaveGSM_TI [10]	21.63	504	2349.40
ForWaRD [21]	25.17	—	—
RI [22]	25.50	—	—

4. EXPERIMENTAL RESULTS AND DISCUSSIONS

In this section, we present a set of two experiments demonstrating the performance of the proposed AALR method in

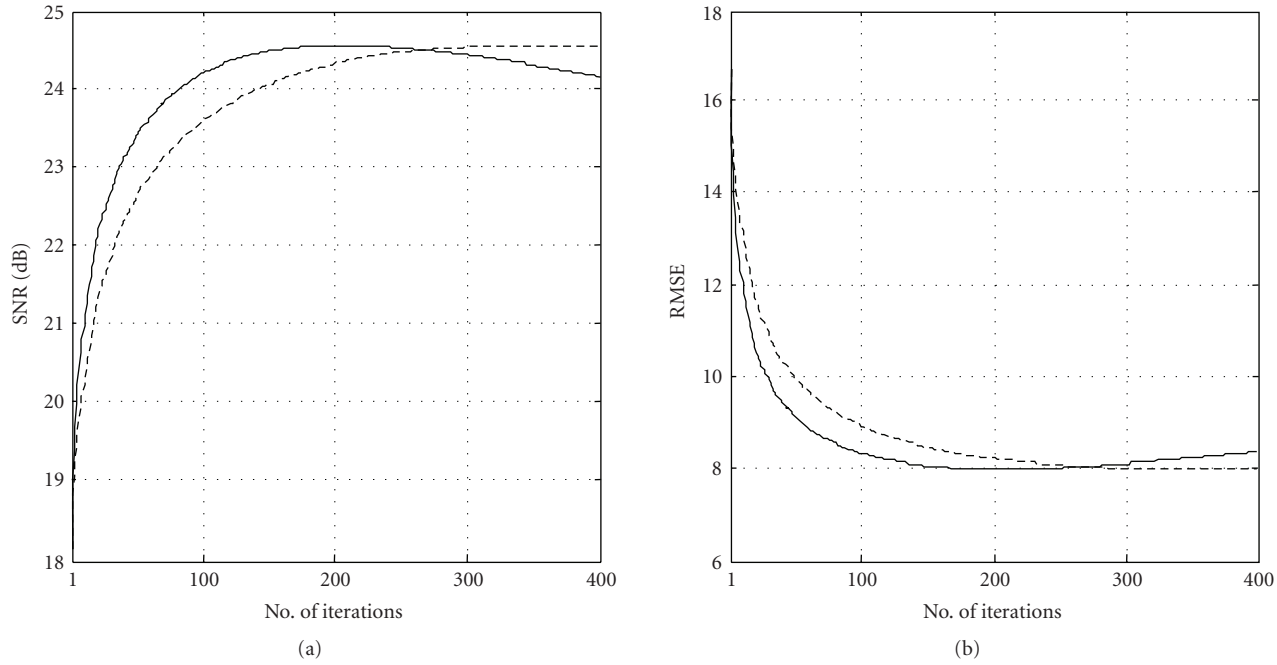

Figure 2: "Cameraman" image: (a) SNR of the LR (dotted line) and SNR of the AALR (solid line); (b) RMSE of the LR (dotted line) and RMSE of the AALR (solid line).

comparison with LR method. Original images are Cameraman (experiment 1) and Lena (experiment 2) both of size 256×256. The corrupting noise is of Poisson type for both experiments. Table 1 displays the blurring PSF, BSNR, and SNR for both experiments. The level of noise in the observed image is characterized in decibels by blurred SNR (BSNR) and defined as [19]

$$\begin{aligned}\mathrm{BSNR} &= 10\log_{10}\left[\sum\left(\overline{H}\overline{x} - (1/MN)\sum\overline{H}\overline{x}\right)^2/\sigma^2 MN\right]\\ &\approx 10\log_{10}\left[\sum\left(\overline{H}\overline{x} - (1/MN)\sum\overline{H}\overline{x}\right)^2/\sum(\overline{y}-\overline{H}\overline{x})^2\right],\end{aligned} \tag{22}$$

σ is the noise standard deviation. The following standard imaging performance criteria are used for the comparison of AALR method and LR method:

$$\begin{aligned}\mathrm{RMSE} &= \sqrt{(1/MN)\sum\left(\overline{x} - \overline{x}^k\right)^2},\\ \mathrm{SNR} &= 10\log_{10}\left(\sum|\overline{x}|^2/\sum|\overline{x} - \overline{x}^k|^2\right).\end{aligned} \tag{23}$$

Most of these criteria actually define the accuracy of approximation of the image intensity function.

Figures 1(c), 1(d) and Figures 3(c), 3(d) show the restored images, corresponding to the maximum SNR, of experiments one and two. It is clear from these figures that the AALR gives almost the same visual results in less number of iterations than LR method for both experiments. Figures 2 and 4 show the variations of SNR and RMSE versus iterations of both experiments. It is observed that the AALR has faster increase in SNR and faster decrease in RMSE in comparison to that of LR method, for both experiments. It is clear that the performance of the proposed AALR method is consistently better than the LR method. In Figures 5(a), and 5(b), it can be seen that the exponent q has value near three at the start of iterations and is approaching to one as iterations increase. Thus, AALR method prefers speed at initial stage of iterations and stability at later stages. It can be observed in Figures 2 and 4 that SNR increases and RMSE decreases up to certain number of iterations and then SNR starts decreasing and RMSE starts increasing. This is due to fact that the noise amplification from one iteration to next iteration is signal-dependent as discussed in Section 3.2. Thus, by using many iterations, there is no guarantee that the quality of the restored image will be better. Thus, to terminate the iterations corresponding to the best result, some stopping criteria must be used [23].

In order to illustrate the superresolution capability of the LR and AALR, we present spectra of the original, blurred, and restored images in Figure 6 for the first experiment. It is evident that the restored spectra, as given in Figures 6(c) and 6(d), have frequency components that are not present in observed spectra as in Figure 6(b). But the restored spectra are not identical to those of the original image spectra as shown in Figure 6(a). In principle, an infinite number of iterations are required to recover the true spectra from the observed spectra using any nonlinear method. But due to noisy observation, noise also gets amplified as the number of iterations increases and the quality of restored image degrades.

Table 2 shows the SNR, number of iterations and computation time of the LR, proposed AALR, WaveGSM_TI [10], ForWaRD [21], and RI [22] algorithms, for experiment 1.

(a) (b)

(c) (d)

Figure 3: "Lenna" image: (a) original image; (b) noisy-blurred image; PSF 5×5 uniform box-car, BSNR $= 32.76$ dB; (c) restored image by LR corresponding maximum SNR in 89 iterations; (d) restored image by AALR corresponding maximum SNR in 52 iterations.

The Matlab implementation of the ForWaRD and the RI is available at http://www.dsp.rice.edu/software/ and http://www.cs.tut.fi/~lasip/#ref_software, respectively.

It is evident from Table 2 that the proposed AALR method performs better in terms of SNR improvement, consumed iterations, and computation time than the other iterative methods. The SNR achieved in AALR method is less than ForWaRD and RI (≈ 1 dB). This is due to the fact that in the ForWaRD and the RI, deblurring is performed followed by denoising. The use of wavelet-domain Wiener filter (WWF) [21, 24] as the postprocessing denoising after deblurring by AALR achieves SNR of 26.10. Thus, our proposed AALR method with WWF yields higher SNR in comparison to other methods.

5. CONCLUSIONS

In this paper, we have proposed an AALR method for image deblurring. In the proposed method, a multiplicative correction term, calculated using an exponent on the correction ratio of conventional LR method, has been used. The proposed empirical technique computes corrective exponent adaptively in each iteration using first-order derivative of the restored image in the previous two iterations. On use of this exponent, the AALR method emphasized speed and stability, respectively, at the early and late stages of iterations. The experimental results were found to support that AALR method gives better results in terms of low RMSE, high SNR, even when 43% of iterations are fewer than conventional LR method. This adaptive method has simple form and can be very easily implemented. Moreover, computations required per iteration in AALR are almost the same as those in conventional LR method. AALR with WWF yields better result, in terms of SNR, than the recently published state-of-the-art methods [10, 21, 22]. An expression for predicting the acceleration step in AALR method has also been derived. The noise amplification and restoration of higher-frequency components, even beyond those present in observed image, result in very complex restoration process. We explained the superresolution property of the accelerated method analytically and verified it experimentally. We have also done analytical analysis of our proposed method, which confirms its signal-dependent noise amplification characteristic.

In the AALR, we have assumed that the PSF is known and shift-invariant. However, in many cases, the PSF is unknown and shift-variant. In such blind deblurring problem,

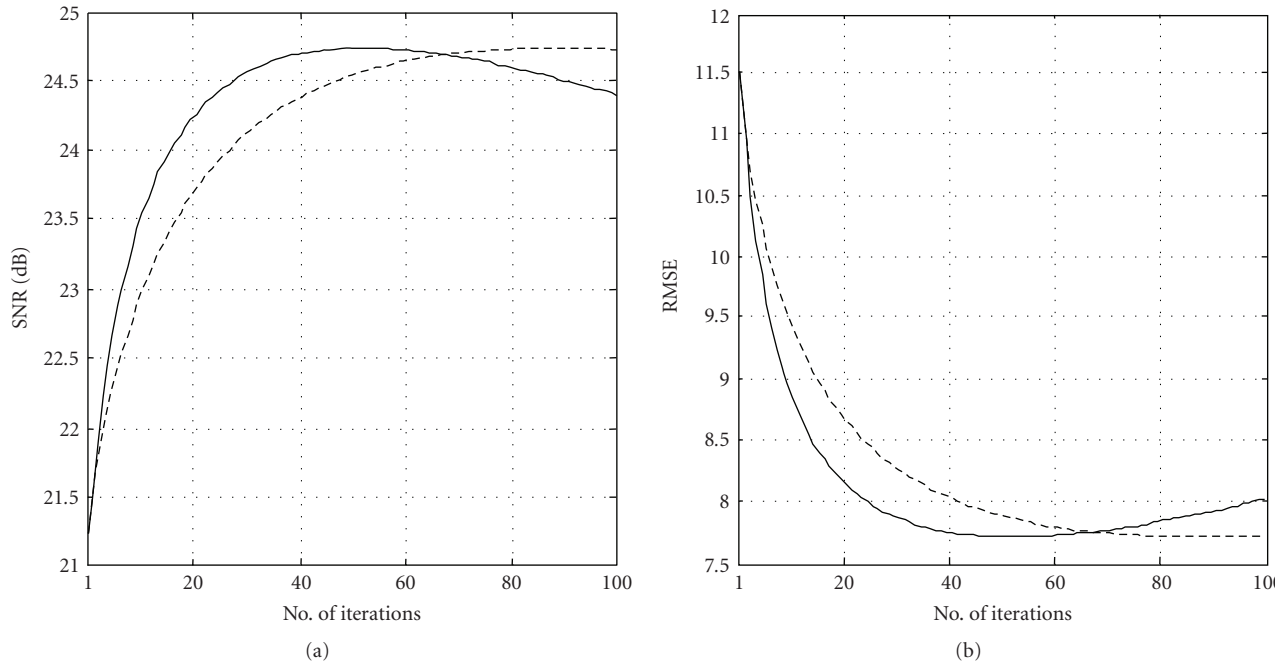

Figure 4: "Lenna" image: (a) SNR of the LR (dotted line); SNR of the AALR (solid line); (b) RMSE of the LR (dotted line), RMSE of the AALR (solid line).

the PSF is estimated from noisy and blurred observations. It is an open problem to extend the proposed AALR method to perform deblurring as well as the estimation of PSF. The proposed AALR method is also not applicable for shift-variant (spatially varying) PSF, however, we are working in this direction.

APPENDIX

DERIVATION OF (21)

For making mathematical step understandable, we rewrite (19) as follows:

$$X^{k+1}(\overline{f}) = X^k(\overline{f}) + Y^k(\overline{f}), \tag{A.1}$$

where

$$Y^k(\overline{f}) = \frac{q}{MN}\sum_{\nu} X^k(\overline{f}-\nu)H^*(\nu)U^k(\nu). \tag{A.2}$$

For estimating noise amplification during iteration, we use covariance analysis. By using covariance, we find the rule of how spatial frequency evolves from one iteration to next iteration. Covariance of X^{k+1} for two different spatial frequencies is given as

$$\begin{aligned}\mu_X^{k+1}(\overline{f},\overline{f}') = E\Big[&\{X^{k+1}(\overline{f}) - E[X^{k+1}(\overline{f})]\}\\ &\times\{X^{k+1}(\overline{f}') - E[X^{k+1}(\overline{f}')]\}^*\Big].\end{aligned} \tag{A.3}$$

Using (A.1) in (A.3) and after the rearrangement of terms, we get the following relation:

$$\begin{aligned}&\mu_X^{k+1}(\overline{f},\overline{f}')\\ &\quad= \mu_X^k(\overline{f},\overline{f}') + \mu_Y^k(\overline{f},\overline{f}') + \mu_{XY^*}^k(\overline{f},\overline{f}') + \mu_{X^*Y}^k(\overline{f},\overline{f}').\end{aligned} \tag{A.4}$$

Using (A.2) and (A.3), we get

$$\begin{aligned}\mu_Y^k(\overline{f},\overline{f}') = &\frac{q^2}{M^2N^2}\sum_{\nu}\sum_{\nu'}\{H(\nu)H^*(\nu')U(\nu)U^{k^*}(\nu')\\ &\times E[X^k(\overline{f}-\nu)X^{k^*}(\overline{f}'-\nu')]\}\\ &-\frac{q^2}{M^2N^2}\sum_{\nu}\sum_{\nu'}\{H(\nu)H^*(\nu')U(\nu)U^{k^*}(\nu')\\ &\times E[X^k(\overline{f}-\nu)]E[X^k(\overline{f}'-\nu')]\},\end{aligned} \tag{A.5}$$

$$\begin{aligned}&\mu_Y^k(\overline{f},\overline{f}')\\ &= \frac{q^2}{M^2N^2}\sum_{\nu}\sum_{\nu'}\{H(\nu)H^*(\nu')U(\nu)U^{k^*}(\nu')\mu_X^k(\overline{f}-\nu,\overline{f}'-\nu')\}.\end{aligned} \tag{A.6}$$

Using (A.2), we get

$$\begin{aligned}&\mu_{XY^*}^k(\overline{f},\overline{f}')\\ &\quad= \frac{q}{MN}\sum_{\nu}\{H(\nu)U^{k^*}(\nu)E[X^k(\overline{f})X^{k^*}(\overline{f}-\nu)]\}\\ &\qquad-\frac{q}{MN}\sum_{\nu}\{H(\nu)U^{k^*}(\nu)E[X^k(\overline{f})]E[X^{k^*}(\overline{f}-\nu)]\}.\end{aligned} \tag{A.7}$$

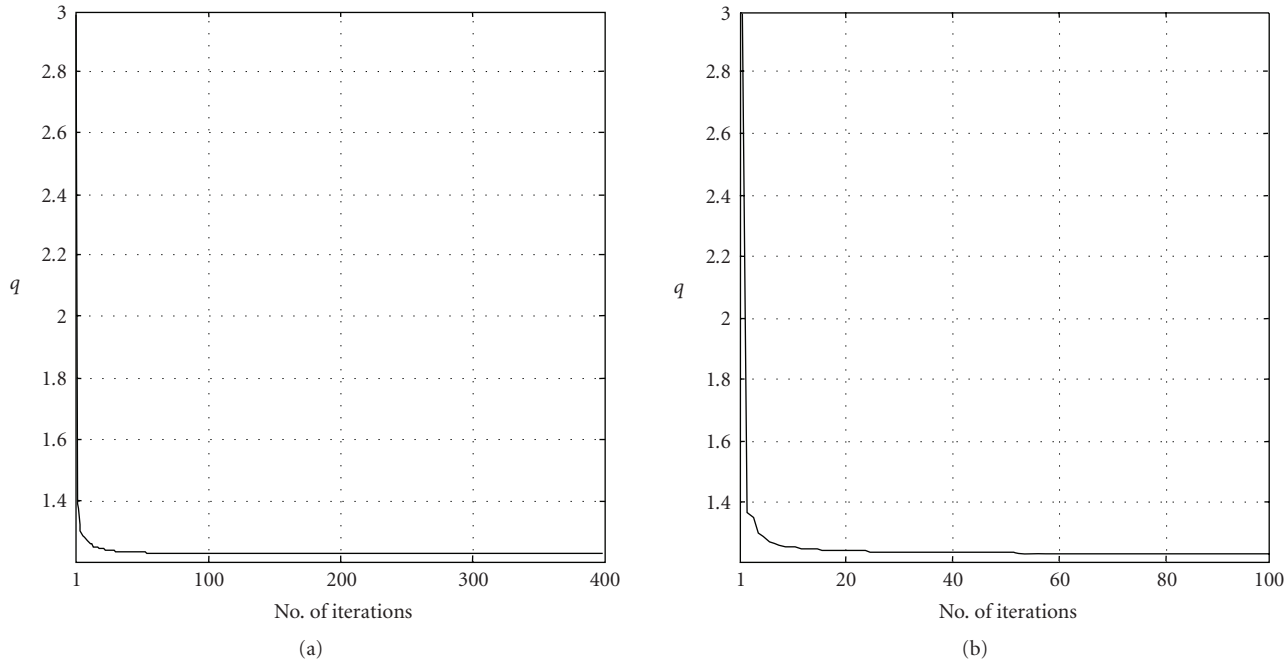

FIGURE 5: Iteration versus q. (a) Cameraman image, (b) Lenna image.

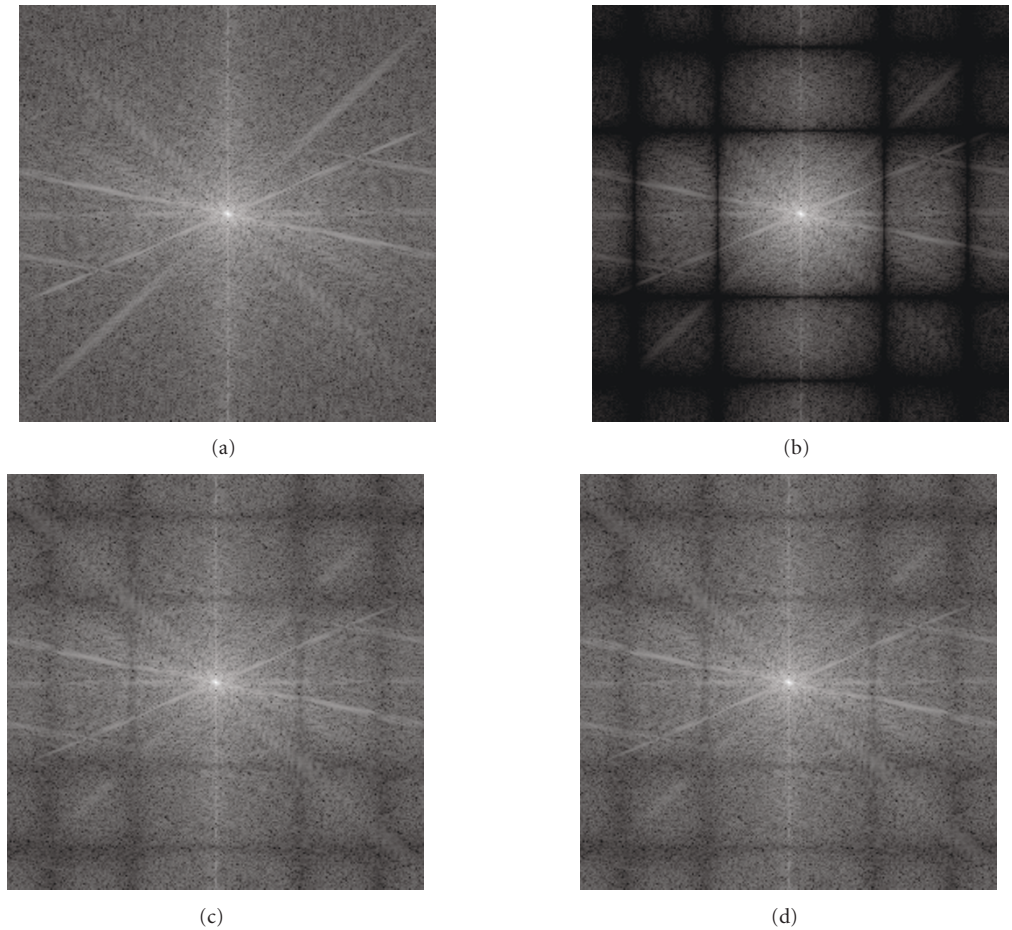

FIGURE 6: Spectra of images from Figure 1. All spectra are range compressed with $\log_{10}(1 + |\cdot|^2)$. (a) Original image in Figure 1(a). (b) Blurred image in Figure 1(b). (c) Figure 1(c). (d) Figure 1(d).

Similarly,

$$\mu^k_{X^*Y}(\overline{f},\overline{f}') = \frac{q}{MN}\sum_{\nu}\{H^*(\nu)U^k(\nu)E[X^{k^*}(\overline{f})X^k(\overline{f}'-\nu)]\} - \frac{q}{MN}\sum_{\nu}\{H^*(\nu)U^k(\nu)E[X^{k^*}(\overline{f})]E[X^k(\overline{f}-\nu)]\}. \tag{A.8}$$

We further assume that one spatial frequency is independent from the other, that is, correlation term at two different spatial frequencies are zero. From (A.4), (A.6), (A.7), and (A.8), we have

$$\mu^{k+1}_X(\overline{f},\overline{f}) = \mu^k_X(\overline{f},\overline{f}) + \frac{q^2}{M^2N^2}\sum_{\nu}|H(\nu)|^2|U^k(\nu)|^2\mu^k_X(\overline{f}-\nu,\overline{f}-\nu) + \frac{2q}{MN}\sum_{\nu}\mathrm{Re}\left(H^*(\nu)U^k(\nu)\right)E\left(|X^k(\overline{f})|^2\right) - \frac{2q}{MN}\sum_{\nu}\mathrm{Re}\left(H^*(\nu)U^k(\nu)\right)|E(X^k(\overline{f}))|^2, \tag{A.9}$$

where Re denotes the real part of complex quantity.

ACKNOWLEDGMENTS

This work was supported by the Dual Use Center through the contract at Gwangju Institute of Science and Technology and by the BK21 program in South Korea.

REFERENCES

[1] A. K. Katsaggelos, *Digital Image Restoration*, Springer, New York, NY, USA, 1989.

[2] A. S. Carasso, "Linear and nonlinear image deblurring: a documented study," *SIAM Journal on Numerical Analysis*, vol. 36, no. 6, pp. 1659–1689, 1999.

[3] P. A. Jansson, *Deconvolution of Images and Spectra*, Academic Press, New York, NY, USA, 1997.

[4] W. H. Richardson, "Bayesian-based iterative method of image restoration," *Journal of the Optical Society of America*, vol. 62, no. 1, pp. 55–59, 1972.

[5] L. B. Lucy, "An iterative techniques for the rectification of observed distributions," *Astronomical Journal*, vol. 79, no. 6, pp. 745–754, 1974.

[6] E. S. Meinel, "Origins of linear and nonlinear recursive restoration algorithms," *Journal of the Optical Society of America A*, vol. 3, no. 6, pp. 787–799, 1986.

[7] J. Nunez and J. Llacer, "A fast Bayesian reconstruction algorithm for emission tomography with entropy prior converging to feasible images," *IEEE Transactions on Medical Imaging*, vol. 9, no. 2, pp. 159–171, 1990.

[8] J. Llacer, E. Veklerov, and J. Nunez, "Preliminary examination of the use of case specific medical information as "prior" in Bayesian reconstruction," in *Proceedings of the 12th International Conference on Information Processing in Medical Imaging (IPMI '91)*, vol. 511 of *Lecture Notes in Computer Science*, pp. 81–93, Wye, UK, July 1991.

[9] M. A. T. Figueiredo and R. D. Nowak, "An EM algorthim for wavelet-besed image restoration," *IEEE Transactions on Image Processing*, vol. 12, no. 8, pp. 906–916, 2003.

[10] J. M. Bioucas-Dias, "Bayesian wavelet-based image donvolution: a GEM algorithm exploiting a class of heavy-tailed priors," *IEEE Transactions on Image Processing*, vol. 15, no. 4, pp. 937–951, 2006.

[11] D. S. C. Biggs and M. Andrews, "Acceleration of iterative image restoration algorithms," *Applied Optics*, vol. 36, no. 8, pp. 1766–1775, 1997.

[12] H. M. Adorf, R. N. Hook, L. B. Luccy, and F. D. Murtagh, "Accelerating the Richardson-Lucy restoration algorithm," in *Proceedings of the 4th ESO/ST-ECF Data Analysis Workshop*, pp. 99–103, Garching, Germany, May 1992.

[13] T. J. Holmes and Y. H. Liu, "Acceleration of maximum-likelihood image restoration for fluorescence microscopy and other noncoherent imagery," *Journal of the Optical Society of America A*, vol. 8, no. 6, pp. 893–907, 1991.

[14] D. S. C. Biggs and M. Andrews, "Conjugate gradient acceleration of maximum-likelihood image restoration," *Electronics Letters*, vol. 31, no. 23, pp. 1985–1986, 1995.

[15] R. G. Lane, "Methods for maximum-likelihood image deconvolution," *Journal of the Optical Society of America A*, vol. 13, no. 6, pp. 1992–1998, 1996.

[16] L. Kaufman, "Implementing and accelerating the EM algorithm for positron emission tomography," *IEEE Transactions on Medical Imaging*, vol. 6, no. 1, pp. 37–51, 1987.

[17] J. A. Fessler and A. O. Hero III, "Space-alternating generalized expectation-maximization algorithm," *IEEE Transactions on Signal Processing*, vol. 42, no. 10, pp. 2664–2677, 1994.

[18] J.-A. Conchello, "Superresolution and convergence properties of the expectation-maximization algorithm for maximum-likelihood deconvolution of incoherent images," *Journal of the Optical Society of America A*, vol. 15, no. 10, pp. 2609–2619, 1998.

[19] V. Katkovnic, K. Egiazarian, and J. Astola, *Local Approximation Techniques in Signal and Image Processing*, SPIE Press, Bellingham, Wash, USA, 2006.

[20] J. G. Proakis and D. G. Manolakis, *Digital Signal Processing, Principles, Algorithms and Applications*, Pearson Education, Singapore, 2004.

[21] R. Neelamani, H. Choi, and R. Baraniuk, "ForWaRD: fourier-wavelet regularized deconvolution for ill-conditioned systems," *IEEE Transactions on Signal Processing*, vol. 52, no. 2, pp. 418–433, 2004.

[22] V. Katkovnik, K. Egiazarian, and J. Astola, "A spatially adaptive nonparametric regression image deblurring," *IEEE Transactions on Image Processing*, vol. 14, no. 10, pp. 1469–1478, 2005.

[23] E. Veklerov and J. Llacer, "Stopping rule for the MLE algorithm based on statistical hypothesis testing," *IEEE Transactions on Medical Imaging*, vol. 6, no. 4, pp. 313–319, 1997.

[24] S. P. Ghael, A. M. Sayeed, and R. G. Baraniuk, "Improved wavelet denoising via empirical Wiener filtering," in *Wavelet Applications in Signal and Image Processing V*, vol. 3169 of *Proceedings of SPIE*, pp. 389–399, San Diego, Calif, USA, July 1997.